

NATIONAL ENERGY TECHNOLOGY LABORATORY



The Importance of Vane Configuration on Yield Stress Measurements of Cement Slurry

14 April 2020



Office of Fossil Energy

DOE/NETL-2020/2116

Disclaimer

This report was prepared as an account of work sponsored by an agency of the United States Government. Neither the United States Government nor any agency thereof, nor any of their employees, makes any warranty, express or implied, or assumes any legal liability or responsibility for the accuracy, completeness, or usefulness of any information, apparatus, product, or process disclosed, or represents that its use would not infringe privately owned rights. Reference therein to any specific commercial product, process, or service by trade name, trademark, manufacturer, or otherwise does not necessarily constitute or imply its endorsement, recommendation, or favoring by the United States Government or any agency thereof. The views and opinions of authors expressed therein do not necessarily state or reflect those of the United States Government or any agency thereof.

Cover Illustration: Vane configurations (2-blade, 3-blade, 4-blade, 6-blade) in the cylindrical arrangement.

Suggested Citation: Tao, C.; Rosenbaum, E.; Kutchko, B.; Massoudi, M. *The Importance of Vane Configuration on Yield Stress Measurements of Cement Slurry*; DOE/NETL-2020/2116; NETL Technical Report Series; U.S. Department of Energy, National Energy Technology Laboratory: Morgantown, WV, 2020; p 24. DOI: 10.18141/1614691.

An electronic version of this report can be found at:

<https://edx.netl.doe.gov/offshore>

The Importance of Vane Configuration on Yield Stress Measurements of Cement Slurry

Chengcheng Tao¹, Eilis Rosenbaum², Barbara Kutchko², Mehrdad Massoudi²

¹ **U.S. Department of Energy, National Energy Technology Laboratory, Oak Ridge Institute for Science and Education, 3610 Collins Ferry Road, Morgantown, WV 26507**

²**U.S. Department of Energy, National Energy Technology Laboratory, 626 Cochran Mill Road, Pittsburgh, PA 15236**

DOE/NETL-2020/2116

14 April 2020

NETL Contacts:

Eilis Rosenbaum, Principal Investigator

Kelly Rose, Technical Portfolio Lead

Bryan Morreale, Executive Director, Research & Innovation Center

This page intentionally left blank.

Table of Contents

ABSTRACT	1
1. INTRODUCTION	2
2. CONSTITUTIVE RELATIONS	3
3. EXPERIMENTAL TECHNIQUES TO MEASURE THE YIELD STRESS	4
4. VANE METHOD FOR CEMENT SLURRY	6
4.1 YIELD STRESS VERSUS TORQUE.....	6
4.2 NORMALIZATION WITH DIRECT SHEAR TEST	11
4.3 SHEAR RATE VERSUS ANGULAR VELOCITY	11
5. CONCLUSIONS	13
6. REFERENCES	15

List of Figures

Figure 1: (a) Lateral view; (b) top view; (c) four-bladed cylindrical vane ($H/D=2.4, 2$ and 1.5)..	6
Figure 2: (a) Lateral view; (b) top view; (c) conical vane ($H/D=2$ and 1.5).....	8
Figure 3: (a) Lateral view; (b) top view; (c) coaxial vane ($H/D=2$ and 1.5).....	9
Figure 4: (a) Lateral view; (b) top view.....	12

List of Tables

Table 1: Summary of the value of K with different vane configurations	10
Table 2: Yield stress τ_0 (Pa)–the absolute value and (the normalized value)–for different pastes with various vane configurations	11

Acronyms, Abbreviations, and Symbols

Term	Description
API	American Petroleum Institute
DOE	U.S. Department of Energy
<i>H/D</i>	Height/diameter ratio
NETL	National Energy Technology Laboratory
WOC	Wait on cement time

Acknowledgments

This work was performed in support of the National Energy Technology Laboratory's (NETL) ongoing research under the Offshore Unconventional Resources – DE FE-1022409 by NETL's Research and Innovation Center. The authors wish to acknowledge Roy Long (NETL Science & Technology Strategic Plans & Programs) and Elena Melchert (DOE Office of Fossil Energy) for programmatic guidance, direction, and support.

The authors also wish to acknowledge the American Petroleum Institute (API) Subcommittee 10, Well Cements for its guidance and collaboration on this important work. The authors wish to offer a special thank you and acknowledgement to the Task Group Chair Glen Bengé, Bengé Consulting, for his guidance, information, and consultation.

This paper is supported by an appointment to the U.S. Department of Energy Postgraduate Research Program for Chengcheng Tao at the National Energy Technology Laboratory, administrated by the Oak Ridge Institute for Science and Education.

ABSTRACT

Vane methods combined with direct shear tests are widely applied to measure the yield stress τ_0 in concentrated suspensions such as cement slurries. This report reviews three different vanes with different shapes and sizes, and examines the relationship between the yield stress versus the torque and the shear rate versus the angular velocity. This research shows that vanes with conical shapes or reduced height/diameter ratio (H/D) result in larger yield stress values.

1. INTRODUCTION

For some non-Newtonian fluids, yield stress is an important rheological parameter (Assaad et al., 2014). Yield stress in cement slurries gives an indication of the ability of the cement to flow and be pumped into the well. Accurately predicting the yield stress for cement slurries, drilling fluids, and concentrated suspensions is important in many industries (Assaad et al., 2016), especially the oil and gas industry. Cement slurries are designed to be pumpable during placement in the well and to then hydrate quickly and develop strength (Watts et al., 2018), thereby reducing wait on cement time (WOC) (Li et al., 2016). Physical testing as well as advanced computational modeling techniques are widely used to study the cement behavior including the mechanical and chemical properties (Ferraro et al., 2017; Tao, 2017; Tao et al., 2019d).

In theory, the yield stress could be obtained from low shear rate tests. The difficulties related to yield stress measurements are discussed in Moller et al. (2009), Dinkgreve et al. (2016), Nguyen and Boger (1992), and Coussot (2014). Coussot (2014) and Coussot et al. (2002) reviewed different methods to measure the yield stress for thixotropic non-Newtonian fluids. Roussel et al. (2012) have suggested two different critical strains in fresh cement pastes: 1) the largest critical strain, which is related to the breakage of the colloidal interactions between cement particles shortly after mixing; 2) the smallest critical strain, which is related to the breakage of the early hydrates. Cement slurries exhibit thixotropic behavior, which can cause different yield stress measurements: 1) the dynamic yield stress measured through the flow curve at equilibrium state (zero shear rate), which is the minimum stress to keep or stop the flow; 2) the static yield stress required to initiate flow starting from rest to the steady state flow before the structure is broken down. The static yield stress, related to the end of elastic behavior and the beginning of plastic deformation is higher than the dynamic yield stress, related to the transition between plastic and viscous flows (Nguyen and Boger, 1992). Both the dynamic and the static stress of fresh cement are measured in a rotational rheometer with vanes (Assaad et al., 2016; Qian and Kawashima, 2018). Michaux and Defosse (1986) indicated that the yield stress of cement slurries exhibited a peak value at low dispersant concentration and decreased to zero at high concentration. The dispersant seemed to break the structure through attractive interparticle forces. To monitor the yield stress condition of the cement slurry in real-time, wireless sensor network-based monitoring systems can be used (Rice et al., 2012; Guan et al., 2014, 2018).

This summary report examines some basic constitutive relations for modeling cement slurries in Section 2. In Section 3, experimental techniques to measure the yield stress are discussed. Section 4 summarizes the vane method for different vane shapes and the height/diameter ratios (H/D) combining with the direct shear test to calculate the yield stress from the torque measurements.

2. CONSTITUTIVE RELATIONS

A recent and detailed review of the constitutive relations for cement slurry is provided by Tao et al. (2020). Cement slurry is considered a non-Newtonian fluid with a yield stress and can be thixotropic (Marchesini et al., 2019; Lootens et al., 2004; Tao et al., 2019b). The Bingham fluid model (Bingham, 1922) is the simplest model to describe a fluid with a yield stress and is widely applied to describe the visco-plastic nature of cement slurries at low shear rates, where

$$\tau = \tau_y + \eta_p \dot{\gamma} \quad (1)$$

where τ is the shear stress, τ_y is the constant yield stress, η_p is the plastic viscosity, and $\dot{\gamma}$ is the shear rate. In addition, the power law model and the Herschel-Bulkley model are also used to describe the relationship between the shear stress and the shear rate: the power law model, proposed by Ostwald (Larson, 1999) describes the fluids with shear-dependent viscosities:

$$\tau = \kappa \dot{\gamma}^n \quad (2)$$

where κ is the consistency factor, n is the flow behavior index (the power-law exponent), measuring the degree of non-Newtonian behavior, and $\dot{\gamma}$ is the shear rate.

Herschel and Bulkley (1926) generalized the Bingham model by introducing a three-parameter model:

$$\tau = \tau_y + \kappa \dot{\gamma}^n \quad (3)$$

where τ_y , κ and n are constants. The measured values of κ are 2.5 or 0.25 and n as 0.75 or 1.25 for cement (Banfill, 2003).

All the above relationships are given in their simple one-dimensional forms. For the full detailed constitutive models, in three-dimensional forms, see Tao et al. (2018, 2019a, 2019c, 2020).

3. EXPERIMENTAL TECHNIQUES TO MEASURE THE YIELD STRESS

Experimental measurements for the yield stress are usually conducted either by direct rheometric techniques or indirect techniques.

Direct techniques are performed by slowly shearing the material and the yield stress is recorded as the peak shear stress when the flow is initiated (Assaad et al., 2014). It measures the yield stress directly instead of using shear stress versus shear rate data. The direct method includes:

- 1) Stress relaxation (Nguyen and Boger, 1983; Fischer et al., 1961): yield stress is the residual stress remaining in the fluid upon the steady state of flow. It is only suitable for fluids with yield stress independent of shear history and has poor reproducibility.
- 2) Creep/recovery experiment (Petrellis and Flumerfelt, 1973; Mewis and Spaul, 1976): when stresses are higher than yield stress, strain increases indefinitely with time without strain recovery and a steady shear rate showing viscous flow is obtained. Some fluids show an obvious change of slope of the creep curve while other fluids are not obvious for yield stress. Imposed stress approaches were applied to the later cases. Yielding could occur at gradually low stresses, due to combining the elastic deformation and viscous flow from breakdown and relaxation (start of irreversible plastic deformation) of fluid under low stress. Only viscous flow occurs at upper yield stress. A new definition for yielding is based on strain instead of stress from the finding that yielding occurs at a constant shear strain, although different yield stress values are obtained. The creep/recovery method is more sensitive and less destructive than other techniques. Creep data should be applied carefully with thixotropic fluids where the yield stress is sensitive to shear history. Also, wall slip, inertia, and damping of the instrument could lead to error for creep data.
- 3) Stress growth experiment (Vinogradov and Malkin, 1980; Speers et al., 1987): shearing a fluid at low and constant shear rate and measure the shear stress as function of time. Three regions are observed on the stress versus time curve: i) initial linear portion for elastic solid behavior; ii) nonlinear curve for stress overshoot, and iii) stress decay region. Different yielding criterion were proposed including the peak shear stress and the point where stress-strain is no longer linear.
- 4) Vane method (Nguyen and Boger, 1983, 1985): measure the peak torque-time response by rotating the vane immersed in the fluid.
- 5) Cone penetration (Moore, 1965; Keentok, 1982): sink a metal cone under constant force into a flat horizontal surface of the fluid. Decrease of shearing area between the cone and fluid results in a graduated decrease in shear stress. The cone stops at some depth when the shear stress equals to yield stress.
- 6) Methods based on static equilibrium of an immersed body (Boardman and Whitmore, 1961).
- 7) Static stability on an inclined plane (Nguyen and Boger, 1992).

The disadvantage of direct techniques for measuring suspension materials like cement include difficult implementation action such as monitoring the shear stress accurately at low shear rates (Ferraris et al., 2001; Nguyen and Boger, 1983; Banfill and Saunders, 1981) and the wall slip effects, which cause under-estimation of the yield stress (Saak et al., 2001; Barnes, 1995).

Indirect techniques are used to determine the yield stress by extrapolating to zero shear rate from a series of shear stress versus shear rate data. The indirect method includes the direct data extrapolation and extrapolation with flow models, such as linear the Bingham model, the nonlinear Casson model, and the Herschel & Bulkley model. The disadvantage of the indirect techniques includes the sensitivity to the model parameters and the experimental data at low shear rates (Ferraris et al., 2001; Banfill and Saunders, 1981).

According to Nguyen and Boger (1992), dynamic mechanical measurements could also be applied to obtain the structural and deformation behavior of viscoplastic fluids at stresses below or near the yield stress. Common techniques include the oscillatory shear testing under sinusoidal deformation of small amplitude. The advantage of this technique is its nondestructive nature with less disturbances for yielding and other rheological behavior. Dynamic behavior at small deformation and large deformation is applied under low stress area as an addition for steady shear measurement.

The ideal yield stress measurement needs a virtual plane of material inside the suspension, where the shearing happens within the material itself other than between the material and an object (Zhang et al., 2010; Assaad et al., 2016). One of the most widely used techniques to measure the yield stress is the vane method since there is no wall slip during the shearing process which happens within the material (Saak et al., 2001; Nguyen and Boger, 1985; Liddel and Boger, 1996). The next sections discuss the vane method.

4. VANE METHOD FOR CEMENT SLURRY

The vane method, originating from soil mechanics and described in detail in ASTM D2573 (ASTM Standard, 2008), has become the standard way of measuring the yield stress τ_0 . The vane consists of two or more blades (4 or more blades provide more consistency in the measurement) and should be fully submerged in the sample material. The yield stress is a function of the vane diameter (D) and height (H) and the vane is rotated at a low enough shear rate so that the maximum torque, T_m , required to initiate flow is then recorded. Following Assaad et al. (2016), this report summarizes their method of determining the relationship between the yield stress and the torque due to the vane geometry as well as the shear rate and angular velocity for vanes with different shapes and with different H/D .

4.1 YIELD STRESS VERSUS TORQUE

This section looks at the relationship of the yield stress and the torque for vanes with four blades and three different blade shapes which sweep: 1) a cylinder, 2) a cone, and 3) a coaxial-cylinder.

4.1.1 Cylindrical Arrangement

For the cylindrical case the vanes have rectangular-shaped blades, which generate a cylindrical volume inside the material. The yielding happens along the periphery of the cylindrical surface. On either side of the cylindrical surface, the un-yielded material exists. Figure 1 shows the configuration of cylindrical vanes with three different height/diameter ratios.

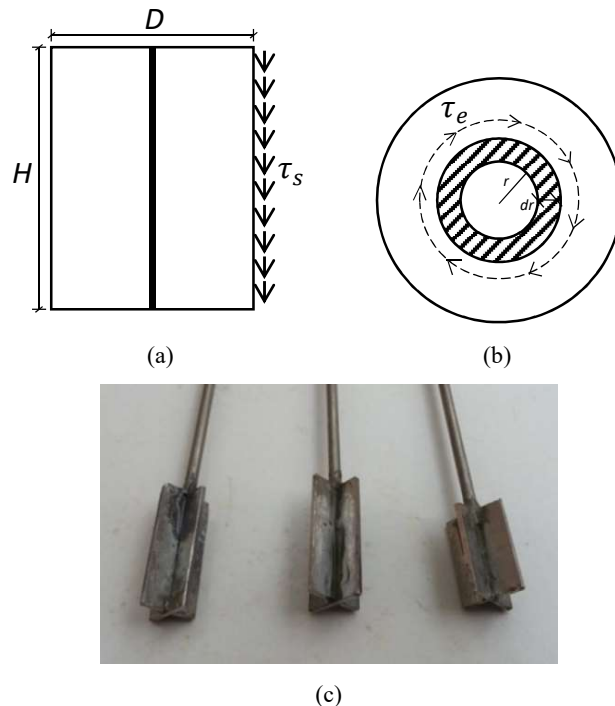


Figure 1: (a) Lateral view; (b) top view; (c) four-bladed cylindrical vane ($H/D=2.4, 2$ and 1.5) (Assaad et al., 2016).

The relationship between the torque T_m and the yield stress τ_0 is:

$$T_m = K\tau_0 \quad (4)$$

where K is a parameter which depends on the geometry of the vane.

The torque, T_s , due to the shear stress at the lateral section, τ_s , is:

$$T_s = \tau_s A_s \frac{D}{2} = \tau_s \cdot (\pi DH) \cdot \frac{D}{2} = \tau_s \frac{\pi D^2 H}{2} \quad (5)$$

The torque, T_e , due to the shear stress at the top and the bottom sections, τ_e , is:

$$T_e = \int_0^R \tau_e 2\pi r dr \cdot r = 2\pi \int_0^{D/2} \tau_e r^2 dr \quad (6)$$

If these two torques are combined (added):

$$T_m = T_s + 2T_e = \tau_s \frac{\pi D^2 H}{2} + 4\pi \int_0^{D/2} \tau_e r^2 dr \quad (7)$$

Assuming that maximum torque occurs on the yield surface, the shear stress at the lateral section τ_s and the shear stress at the top and the bottom sections τ_e equal the yield stress τ_0 , where $\tau_e = \tau_s = \tau_0$, then:

$$T_m = \tau_0 \cdot \frac{\pi D^2 H}{2} + 4\pi \int_0^{D/2} \tau_0 r^2 dr = \tau_0 \left[\left(\frac{\pi D^3}{2} \right) \left(\frac{H}{D} + \frac{1}{3} \right) \right] = K\tau_0 \quad (8)$$

where the quantity in the bracket can be defined as K appearing in Equation (4):

$$K_{cylinder} = \left(\frac{\pi D^3}{2} \right) \left(\frac{H}{D} + \frac{1}{3} \right) \quad (9)$$

$K_{cylinder}$ for the four-bladed vanes shown in Figure 1 are as follows:

Four-bladed vane with H/D of 2.4 ($H=24\text{mm}$, $D=10\text{mm}$), $K_{cylinder}=4.29 \times 10^{-6}\text{m}^3$

Four-bladed vane with H/D of 2 ($H=24\text{mm}$, $D=12\text{mm}$), $K_{cylinder}=6.33 \times 10^{-6}\text{m}^3$

Four-bladed vane with H/D of 1.5 ($H=18\text{mm}$, $D=12\text{mm}$), $K_{cylinder}=4.97 \times 10^{-6}\text{m}^3$

In these examples from Assaad et al. (2016), $K_{cylinder}$ is the largest at the ratio H/D of 2 for the four-bladed cylindrical vane.

4.1.2 Conical Case

Figure 2 shows the configuration of conical vanes with two different H/D . The vanes have triangle-shaped blades, which shear a conical volume inside the material.

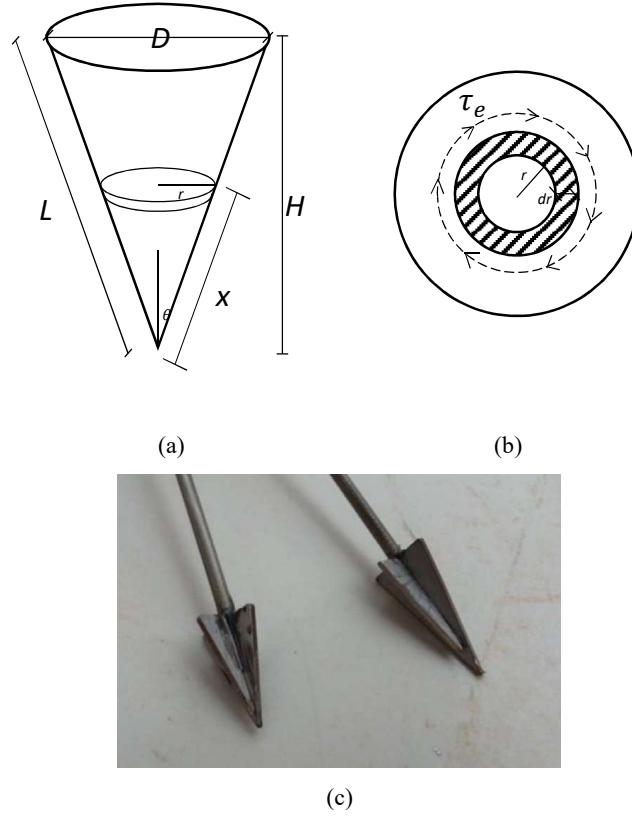


Figure 2: (a) Lateral view; (b) top view; (c) conical vane ($H/D=2$ and 1.5) (Assaad et al., 2016).

The torque T_s due to the shear stress τ_s at a lateral section is:

$$T_s = \int_0^L 2\pi r dx \cdot \tau_s x \tan\theta \quad (10)$$

Now, $r = x \sin\theta = x \frac{D}{2L}$, thus,

$$T_s = \frac{\pi D}{L} \tan\theta \tau_s \int_0^L x^2 dx \quad (11)$$

where x is the distance varying from 0 to L (see Figure 2(a) for notations).

The torque, T_e , due to the shear stress, τ_e , at the top is:

$$T_e = \int_0^{D/2} \tau_e 2\pi r dr \cdot r = 2\pi \int_0^{D/2} \tau_e r^2 dr \quad (12)$$

Assuming that at maximum torque, the shear stress at the lateral section, τ_s , and the shear stress at the top and the bottom sections, τ_e , is equal to the yield stress τ_0 , where $\tau_e = \tau_s = \tau_0$:

$$T_m = T_s + T_e = \frac{\pi D}{L} \tan\theta \tau_0 \frac{L^3}{3} + 2\pi\tau_0 \frac{(D/2)^3}{3} = \frac{\pi D}{3} \left(\frac{D^2}{4} + L^2 \tan\theta \right) \tau_0 \quad (13)$$

Where the geometric parameter, K , in Equation (4) is now given by:

$$K_{cone} = \left(\frac{\pi D}{3} \right) \left(\frac{D^2}{4} + L^2 \tan\theta \right) \quad (14)$$

The values of K_{cone} for conical vanes shown in Figure 2 are as follows:

Conical vane with H/D of 2 ($H=24\text{mm}$, $D=12\text{mm}$), $K_{cone}=2.31 \times 10^{-6}\text{m}^3$

Conical vane with H/D of 1.5 ($H=18\text{mm}$, $D=12\text{mm}$), $K_{cone}=1.88 \times 10^{-6}\text{m}^3$

Coaxial-cylindrical case

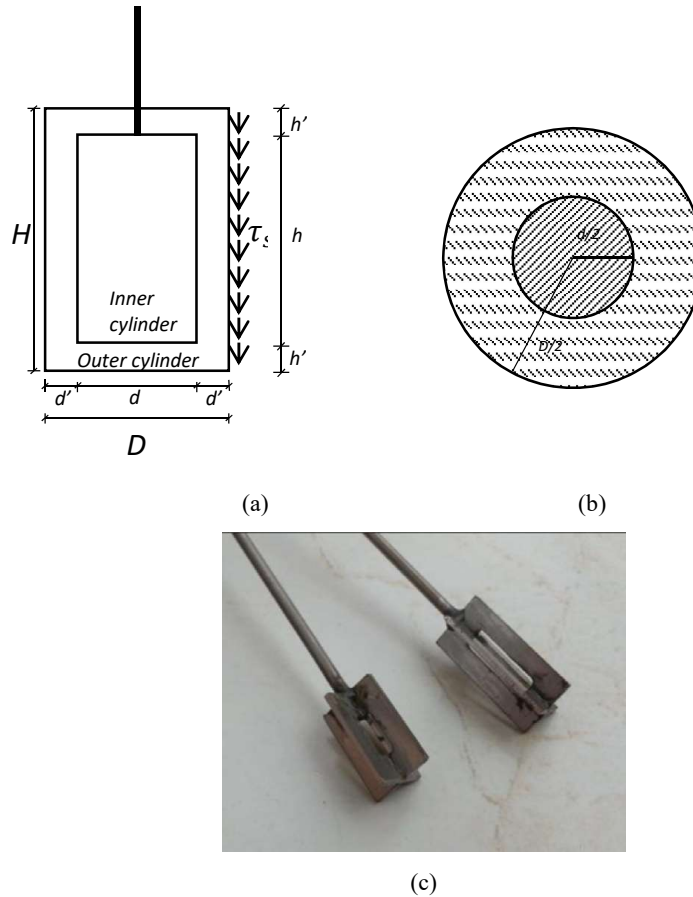


Figure 3: (a) Lateral view; (b) top view; (c) coaxial vane ($H/D=2$ and 1.5) (Assaad et al., 2016).

Figure 3 shows the configuration for the coaxial vanes with two different height/diameter ratios. The vanes have slotted rectangular-shaped blades, which shear a coaxial cylindrical volume inside the material.

The torque, T_s , due to the shear stress, τ_s , at a lateral section is:

$$T_s = \pi D \cdot 2h' \left(\frac{D}{2}\right) \tau_s + \pi D h \left(\frac{D}{2}\right) \tau_s - \pi d h \left(\frac{d}{2}\right) \tau_s \quad (15)$$

The torque, T_e , due to the shear stress, τ_e , on the top and the bottom sections is:

$$T_e = 2\pi \int_0^{D/2} \tau_e r^2 dr + 2\pi \int_0^{d/2} \tau_e r^2 dr \quad (16)$$

If these two torques are added then:

$$T_m = T_s + 2T_e \quad (17)$$

Assuming that at maximum torque, the shear stress at the lateral section, τ_s , and the shear stress at the top and the bottom sections, τ_e , are equal to the yield stress, τ_0 , where $\tau_e = \tau_s = \tau_0$, then:

$$T_m = \left[\frac{1}{2} \pi D^2 H - \frac{1}{2} \pi d^2 h + \frac{\pi}{6} (D^3 + d^3) \right] \tau_0 = \left[\frac{\pi D^3}{2} \left(\frac{H}{D} + \frac{1}{3} \right) + \frac{\pi d^3}{2} \left(\frac{1}{3} - \frac{h}{d} \right) \right] \tau_0 \quad (18)$$

where the geometric parameter, K , in Equation (4) is now given by:

$$K_{coaxial} = \left[\frac{\pi D^3}{2} \left(\frac{H}{D} + \frac{1}{3} \right) + \frac{\pi d^3}{2} \left(\frac{1}{3} - \frac{h}{d} \right) \right] \quad (19)$$

For the coaxial-cylindrical vanes shown in Figure 3, the $K_{coaxial}$ are calculated as follows:

Slotted vane with H/D of 2 ($H=24\text{mm}$, $D=12\text{mm}$, $h=12\text{mm}$, $d=4\text{mm}$), $K_{coaxial}=5.5 \times 10^{-6}\text{m}^3$

Slotted vane with H/D of 1.5 ($H=18\text{mm}$, $D=12\text{mm}$, $h=8\text{mm}$, $d=4\text{mm}$), $K_{coaxial}=4.4 \times 10^{-6}\text{m}^3$

A summary of the equations that define K for three vane configurations as a function of the H/D is given in Table 1.

Table 1: Summary of the value of K with different vane configurations

Vane Configuration	Relationship between T_m and τ_0
Cylindrical vane	$K_{cylinder} = \left(\frac{\pi D^3}{2} \right) \left(\frac{H}{D} + \frac{1}{3} \right)$
Conical vane	$K_{cone} = \left(\frac{\pi D}{3} \right) \left(\frac{D^2}{4} + L^2 \tan \theta \right)$
Coaxial vane	$K_{coaxial} = \left[\frac{\pi D^3}{2} \left(\frac{H}{D} + \frac{1}{3} \right) + \frac{\pi d^3}{2} \left(\frac{1}{3} - \frac{h}{d} \right) \right]$

4.2 NORMALIZATION WITH DIRECT SHEAR TEST

The vane method is applied to measure the absolute value of the yield stress (τ_0). Assaad (2016) conducted measurements on cement pastes using a direct shear test to determine the shear strength property, cohesion (C). Due to the relatively limited ranges of responses and variability within test data, τ_0 was normalized with a corresponding C value from direct shear tests. The normalized yield stress is:

$$|\tau_0| = \frac{\tau_0 - C}{C} \times 100 \quad (20)$$

Table 2 shows the absolute value of the yield stress and the normalized yield stress for different cement pastes with various vane configurations. The direct shear test data is taken from Assaad's data (Assaad et al., 2016).

Table 2: Yield stress τ_0 (Pa)–the absolute value and (the normalized value)–for different pastes with various vane configurations

Cement Paste	C(Pa)	4-Blade Cylindrical Vane			Conical Vane		Coaxial Vane	
		H/D=2.4	H/D=2	H/D=1.5	H/D=2	H/D=1.5	H/D=2	H/D=1.5
Paste #1	559.5	731.4 (30.72)	768.2 (37.3)	754.4 (34.83)	756.2 (35.16)	792.5 (41.64)	710.7 (27.02)	702.3 (25.52)
Paste #2	473	612 (29.39)	604.5 (27.8)	670 (41.65)	692.5 (46.41)	742 (56.87)	563 (19.03)	571 (20.72)
Paste #3	326.8	451.8 (38.25)	462 (41.37)	510.3 (56.15)	482 (47.49)	507.6 (55.32)	448.8 (37.33)	490.8 (50.18)
Paste #4	197	237.4 (20.51)	260.1 (32.03)	273 (38.58)	266 (35.03)	281.7 (42.99)	223.7 (13.55)	236.2 (19.90)
Paste #5	168.3	203.6 (20.97)	200.5 (19.13)	226.9 (34.82)	189.6 (12.66)	213 (26.56)	192.7 (14.50)	209 (24.18)
Paste #6	91.2	121.9 (33.66)	133.2 (46.05)	117.7 (29.06)	134 (46.93)	152 (66.67)	128 (40.35)	121.2 (32.89)
Paste #7	43.5	58.1 (33.56)	56 (28.74)	54.8 (25.98)	62.3 (43.22)	63.9 (46.90)	53.6 (23.22)	52 (19.54)

4.3 SHEAR RATE VERSUS ANGULAR VELOCITY

This section looks at the relationship between the rotation speed (known as angular velocity, Ω) of the vane and the rate of shearing ($\dot{\gamma}$) along coaxial-cylinders rheometer for cement slurry (Lanos and Estellé, 2016). Lano's method (Lanos and Estellé, 2016) was applied for this calculation, which generates more accurate flow curves than other methods assuming a

homogeneous shear. It is assumed that the outer cylinder is equivalent to the inner wall of the rheometer with the radius R_e and the vane, which generates the inner cylinder with the radius R_i . Two cases, including the fully and not fully sheared gap between cylinders, are considered in the calculation. The fluid is considered as the Bingham fluid model with yield stress τ_0 . Figure 4 shows the configuration for the coaxial vanes at lateral view and top view for the shear rate calculation. The vanes have slotted rectangular-shaped blades, which cut a coaxial cylindrical volume inside the material.

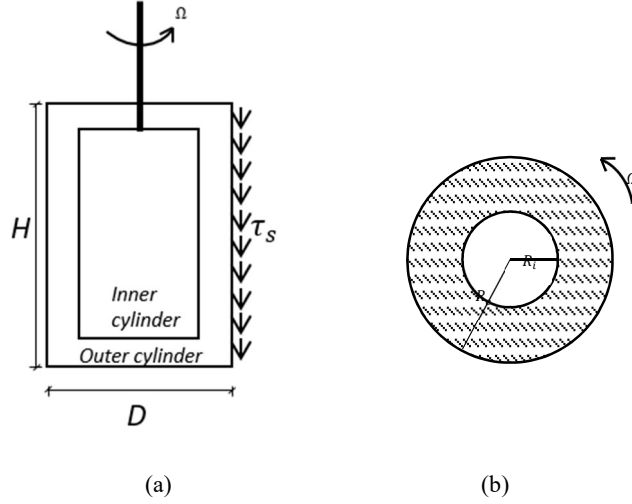


Figure 4: (a) Lateral view; (b) top view.

The angular velocity Ω is calculated as:

$$\Omega = \int_{R_i}^r \frac{d\omega}{dr} dr = \int \frac{\dot{\gamma}}{r} dr = \int_{R_i}^r \frac{\tau(r) - \tau_0}{\mu r} dr = \frac{\tau - \tau(r)}{2\mu} - \frac{\tau_0}{\mu} \ln\left(\frac{r}{R_i}\right) \quad (21)$$

where μ is the plastic viscosity and τ_0 is the yield stress.

For the case of the partially sheared gap, $\tau < \tau_0 \frac{R_e^2}{R_i^2}$, and the shear rate is:

$$\dot{\gamma} = \frac{2\Omega}{1 - \frac{\tau_0}{\tau - \tau_0} \ln\left(\frac{\tau}{\tau_0}\right)} \quad (22)$$

For the case of the fully sheared gap, $\tau > \tau_0 \frac{R_e^2}{R_i^2}$, and the shear rate is:

$$\dot{\gamma} = 2\Omega + \frac{2\tau_0}{\mu} \ln\left(\frac{R_e}{R_i}\right) + \frac{\tau}{\mu} \left(\frac{R_i}{R_e}\right)^2 - \frac{\tau_0}{\mu} \quad (23)$$

5. CONCLUSIONS

Yield stress indicates the ability of a material to flow, an important rheological property for multiple applications. Cement is a fluid/particle system that is typically considered to have a yield stress. Cement is used in the oil and gas industry to isolate the well—it needs to be pumpable during placement in the well and needs to harden quickly after placement to prevent formation fluids from migrating through the cement. It is important to determine the best method to measure yield stress and the influence of the method on the results. The vane method is a widely acceptable method to measure yield stress as it eliminates wall slip, an issue with some methods which can introduce error into the measurement.

Various vane configurations are used in commercial instruments. This report compiled the results of a literature review of several common vane configurations on the yield stress measurement for cement pastes. The values of the yield stress are shown for standard generic shapes: cylindrical, conical, and coaxial-cylindrical cases with different H/D . The direct shear test can be used to normalize the calculated yield stress from the vane method. The normalized data has a lower standard deviation when compared to the data that was not normalized; therefore, if the direct shear test can be administered, it would be beneficial to normalize the results. A typical direct shear device designed for measuring soils must be retrofitted in order to measure cement slurries, which have an initial low yield stress at early times after mixing (which initiates the hydration process). Direct shear devices are typically used to measure the yield stress of soils with low water content. This report examined the relationship between shear rate and angular velocity for the coaxial-cylinder case. These relationships provide guides for the petroleum and cement industry when conducting similar tests.

This page intentionally left blank.

6. REFERENCES

- ASMT Standard. D2573 Standard Test Method for Field Vane Shear Test in Cohesive Soil, 2008.
- Assaad, J. J.; Harb, J.; Maalouf, Y. Effect of Vane Configuration on Yield Stress Measurements of Cement Pastes. *Journal of Non-Newtonian Fluid Mechanics* **2016**, *230*, 31–42.
- Assaad, J. J.; Harb, J.; Maalouf, Y. Measurement of Yield Stress of Cement Pastes Using the Direct Shear Test. *Journal of Non-Newtonian Fluid Mechanics* **2014**, *214*, 18–27.
- Banfill, P. F. G. The Rheology of Fresh Cement and Concrete-a Review. In Proceedings of the 11th International Cement Chemistry Congress, 2003; p. 50–62.
- Banfill, P. F. G.; Saunders, D. C. On the Viscometric Examination of Cement Pastes. *Cement and Concrete Research* **1981**, *11*, 363–70.
- Barnes, H. A. A Review of the Slip (Wall Depletion) of Polymer Solutions, Emulsions and Particle Suspensions in Viscometers: Its Cause, Character, and Cure. *Journal of Non-Newtonian Fluid Mechanics* **1995**, *56*, 221–51.
- Bingham, E. C. Fluidity and Plasticity. McGraw-Hill; 1922; Vol. 2.
- Boardman, G.; Whitmore, R. L. The Static Measurement of Yield Stress. *Lab. Pract* **1961**, *10*, 782–85.
- Coussot, P. Yield Stress Fluid Flows: A Review of Experimental Data. *Journal of Non-Newtonian Fluid Mechanics* **2014**, *211*, 31–49.
- Coussot, P.; Nguyen, Q. D.; Huynh, H. T.; Bonn, D. Viscosity Bifurcation in Thixotropic, Yielding Fluids. *Journal of Rheology* **2002**, *46*, 573–89.
- Dinkgreve, M.; Paredes, J.; Denn, M. M.; Bonn, D. On Different Ways of Measuring ‘the’ Yield Stress. *Journal of Non-Newtonian Fluid Mechanics* **2016**, *238*, 233–41.
- Ferraris, C. F.; Brower, L. E.; Banfill, P.; Beaupré, D.; Chapdelaine, F.; de Larrard, F.; Domone, P. Comparison of Concrete Rheometers: International Test at LCPC (Nantes, France) in October, 2000. US Department of Commerce, National Institute of Standards and Technology, 2001.
- Ferraro, C. C.; Watts, B.; Tao, C.; Masters, F. *Advanced Analysis, Validation and Optimization of Virtual Cement and Concrete Testing*; 2017.
- Fischer, W. H.; Bauer, W. H.; Wiberley, S. E. 1961. Yield Stresses and Flow Properties of Carboxypolymethylene-Water Systems. *Transactions of the Society of Rheology* **1961**, *5*, 221–35.
- Guan, S.; Bridge, J. A.; Li, C.; DeMello, N. J. Smart Radar Sensor Network for Bridge Displacement Monitoring. *Journal of Bridge Engineering* **2018**, *23*, 04018102.
- Guan, S.; Rice, J. A.; Li, C.; Gu, C. Automated DC Offset Calibration Strategy for Structural Health Monitoring Based on Portable CW Radar Sensor. *IEEE Transactions on Instrumentation and Measurement* **2014**, *63*, 3111–18.
- Herschel, W. H., and Ronald Bulkley. 1926. “Measurement of Consistency as Applied to Rubber-Benzene Solutions.” In Am. Soc. Test Proc, 26:621–33.

- Keentok, M. The Measurement of the Yield Stress of Liquids. *Rheologica Acta* **1982**, *21*, 325–32.
- Lanos, C.; Estellé, P. *CC Flow Curves from Vane Geometry Rheometer*; 2016.
- Larson, R. G. *The Structure and Rheology of Complex Fluids*; Oxford University press New York, 1999; Vol. 150.
- Li, Z.; Vandebossche, J.; Iannacchione, A.; Brigham, J.; Kutcho, B. Theory-Based Review of Limitations With Static Gel Strength in Cement/Matrix Characterization. *SPE Drilling & Completion* **2016**, *31*, 145–58.
- Liddel, P. V.; Boger, D. V. Yield Stress Measurements with the Vane. *Journal of Non-Newtonian Fluid Mechanics* **1996**, *63*, 235–61.
- Lootens, D.; Hébraud, P.; Lécolier, E.; Van Damme, H. Gelation, Shear-Thinning and Shear-Thickening in Cement Slurries. *Oil & Gas Science and Technology* **2004**, *59*, 31–40.
- Marchesini, F. H.; Oliveira, R. M.; Althoff, H.; de Souza Mendes, P. R. Irreversible Time-Dependent Rheological Behavior of Cement Slurries: Constitutive Model and Experiments. *Journal of Rheology* **2019**, *63*, 247–62.
- Mewis, J.; Spaul, A. J. B. 1976. Rheology of Concentrated Dispersions. *Advances in Colloid and Interface Science* **1976**, *6*, 173–200.
- Michaux, M.; Defosse, C. Oil Well Cement Slurries I. Microstructural Approach of Their Rheology. *Cement and Concrete Research* **1986**, *16*, 23–30.
- Moller, P.; Fall, A.; Chikkadi, V.; Derks, D.; Bonn, D. An Attempt to Categorize Yield Stress Fluid Behaviour. *Philosophical Transactions of the Royal Society A: Mathematical, Physical and Engineering Sciences* **2009**, *367*, 5139–55.
- Moore, F. *Rheology of Ceramic Systems*; Elsevier; 1965.
- Nguyen, Q. D.; Boger, D. V. Direct Yield Stress Measurement with the Vane Method. *Journal of Rheology* **1985**, *29*, 335–47.
- Nguyen, Q. D.; Boger, D. V. Measuring the Flow Properties of Yield Stress Fluids. *Annual Review of Fluid Mechanics* **1992**, *24*, 47–88.
- Nguyen, Q. D.; Boger, D. V. Yield Stress Measurement for Concentrated Suspensions. *Journal of Rheology* **1983**, *27*, 321–49. <https://doi.org/10.1122/1.549709>
- Petrellis, N. C.; R. W. Flumerfelt, R. W. Rheological Behavior of Shear Degradable Oils: Kinetic and Equilibrium Properties. *The Canadian Journal of Chemical Engineering* **1973**, *51*, 291–301.
- Qian, Y.; Kawashima, S. Distinguishing Dynamic and Static Yield Stress of Fresh Cement Mortars through Thixotropy. *Cement and Concrete Composites* **2018**, *86*, 288–96.
- Rice, J. A.; Gu, C.; Li, C.; Guan, S. A Radar-Based Sensor Network for Bridge Displacement Measurements. In *Sensors and Smart Structures Technologies for Civil, Mechanical, and Aerospace Systems*; International Society for Optics and Photonics, 2012; 8345:83450I.
- Roussel, N.; Ovarlez, G.; Garrault, S.; Brumaud, C. The Origins of Thixotropy of Fresh Cement Pastes. *Cement and Concrete Research* **2012**, *42*, 148–57.

- Saak, A. W.; Jennings, H. M.; Shah, S. P. The Influence of Wall Slip on Yield Stress and Viscoelastic Measurements of Cement Paste. *Cement and Concrete Research* **2001**, *31*, 205–12.
- Speers, R. A.; Holme, K. R.; Tung, M. A.; Williamson, W. T. Drilling Fluid Shear Stress Overshoot Behavior. *Rheologica Acta* **1987**, *26*, 447–52.
- Tao, C. Optimization of Cement Production and Hydration for Improved Performance, Energy, Conservation, and Cost. Ph.D. Dissertation, University of Florida, 2017.
- Tao, C.; Kutchko, B. G.; Rosenbaum, E.; Massoudi, M. A Review of Rheological Modeling of Cement Slurry in Oil Well Applications. *Energies* **2020**, *13*, 570.
- Tao, C.; Kutchko, B. G.; Rosenbaum, E.; Wu, W.-T.; Massoudi, M. Steady Flow of a Cement Slurry. *Energies* **2019a**, *12*, 2604.
- Tao, C.; Rosenbaum, E.; Kutchko, B. G.; Massoudi, M. *Effects of Shear-Rate Dependent Viscosity on the Flow of a Cement Slurry*; No. NETL-PUB-22169; National Energy Technology Laboratory, 2018.
- Tao, C.; Rosenbaum, E.; Kutchko, B. G.; Massoudi, M. *Flow of a Cement Slurry Modeled as a Generalized Second Grade Fluid (ASME-JSME-KSME Joint Fluids Engineering Conference)*; No. NETL-PUB-22384; National Energy Technology Laboratory, 2019b.
- Tao, C.; Rosenbaum, E.; Kutchko, B. G.; Massoudi, M. *Steady and Transient Flow of a Cement Slurry*; No. NETL-PUB-22383; National Energy Technology Laboratory, 2019c.
- Tao, C.; Watts, B.; Ferraro, C. C.; Masters, F. J. A Multivariate Computational Framework to Characterize and Rate Virtual Portland Cements. *Computer-Aided Civil and Infrastructure Engineering* **2019d**, *34*, 266–78.
- Vinogradov, G. V.; Malkin, A. J. Rheology of Polymers.(Reologi [j] a Polimerov). Viscoelasticity and Flow of Polymers.(Transl. by Artavaz Beknazarov). Mir-Springer XII; 1980.
- Watts, B. E.; Tao, C.; Ferraro, C. C.; Masters, F. J. Proficiency Analysis of VCCTL Results for Heat of Hydration and Mortar Cube Strength. *Construction and Building Materials* **2018**, *161*, 606–617.
- Zhang, M.-H.; Chiara F. Ferraris, C. F.; Zhu, H.; Picandet, V.; Peltz, M. A.; Stutzman, P.; De Kee, D. Measurement of Yield Stress for Concentrated Suspensions Using a Plate Device. *Materials and Structures* **2010**, *43*, 47–62.

This page intentionally left blank.



Brian J. Anderson

Director
National Energy Technology Laboratory
U.S. Department of Energy

John Wimer

Associate Director
Strategic Planning
Science & Technology Strategic Plans
& Programs
National Energy Technology Laboratory
U.S. Department of Energy

Roy Long

Technology Manager
Science & Technology Strategic Plans
& Programs
National Energy Technology Laboratory
U.S. Department of Energy

Elena Melchert

Director
Division of Upstream Oil and Gas
Research
U.S. Department of Energy

Bryan Morreale

Executive Director
Research and Innovation Center
National Energy Technology Laboratory
U.S. Department of Energy